JOURNAL OF MATERIALS SCIENCE **34** (1999) 3275–3280

Thermal behavior of α-$Ba(FeS_2)_2$ and $AgFeS_2$: quasi-unidimensional and 3D network compounds prepared from ion-exchange on the same precursor

A. GALEMBECK, O. L. ALVES
Laboratório de Química do Estado Sólido, Instituto de Química—UNICAMP, Caixa Postal 6154, CEP 13081-970, Campinas-SP, Brazil
E-mail: oalves@iqm.unicamp.br

Thermal behavior of $AgFeS_2$ and α-$Ba(FeS_2)_2$ were studied under air atmosphere. Decomposition products of $AgFeS_2$ are Ag_2S, FeS_2 (pyrite form), Ag_2SO_4, α-Fe_2O_3 and metallic silver. α-$Ba(FeS_2)_2$ decomposes to pyrite, α-Fe_2O_3 and $BaSO_4$. We propose that metallic sulfide formation on the initial step of the decomposition of these compounds is related to the packing of the metallic ions with sulfur and, hence, with metal-sulfur distances in the original material. Morphological information about $AgFeS_2$ and α-$Ba(FeS_2)_2$ are presented for the first time.

1. Introduction

$KFeS_2$ presents a linear $(FeS_2)_n^{n-}$ chain structure with an antiferromagnetic iron-iron coupling and a strong covalent character in the Fe-S bonds. The chain-chain distance is 6.50 Å, potassium ions lying among them [1]. Quasi-unidimensional antiferromagnets, like this, show unusual physical and chemical properties. This makes this compound into an interesting research topic in widely separated areas, such as magnetism, biochemistry and electrochemistry [2–5].

The structural features of $KFeS_2$ allow the alkali metal to be exchanged by other metallic ions. Two kinds of reaction may occur: (i) ion-exchange by alkaline-earth ions like Sr^{2+} or Ba^{2+}, in which case the chain structure remains unchanged, but some rearrangement proceeds to accommodate the bivalent cations [6], and (ii) ion-exchange by Ag^+ and Cu^+ with diffusion of alternating iron atoms out of the tetrahedra and a complete breakdown of the chain structure, leading to a three-dimensional network with chalcopyrite structure, all atoms lying on tetrahedral sites [7, 8].

The use of $KFeS_2$ as a precursor is the only way to synthesize compounds like α-$Ba(FeS_2)_2$ and $AgFeS_2$ [7, 9]. In this work, we present data on the thermal behavior of the $KFeS_2$ derivatives with the two kinds of structure described above: α-$Ba(FeS_2)_2$, which is a chain compound, and $AgFeS_2$, a three-dimensional network, isostructural with chalcopyrite.

2. Experimental

2.1. Preparation of $KFeS_2$

Polycrystalline $KFeS_2$ was prepared by the method described in our earlier paper and identified by X-ray diffraction (XRD) [10].

2.2. Preparation of α-$Ba(FeS_2)_2$

Polycrystalline samples of α-$Ba(FeS_2)_2$ were obtained by the method of Boller [6], by reacting $KFeS_2$ with a 0.25M $Ba(NO_3)_2$ aqueous solution in a closed system under nitrogen atmosphere, using Schlenk glass apparatus, at room temperature for 8 hours. The compound was identified by XRD and chemical analysis by X-ray fluorescence (XRF).

2.3. Preparation of $AgFeS_2$

Polycrystalline $AgFeS_2$ was synthesized following the method by Boon [7], by reacting $KFeS_2$ with a 0.25M $AgNO_3$ aqueous solution under air atmosphere at room temperature for 1.5 hour. The compound was identified by XRD and the amount of silver was determined by titration with KSCN.

2.4. Heat treatment

The samples (0.25 g) were heated within a horizontal furnace for 2 hours, in static heat treatments, under air atmosphere, at temperatures ranging from 100 to 1000 °C and cooled to room temperature.

2.5. Physical measurements

XRD patterns were obtained using a Shimadzu, model XD-3A, diffractometer with Ni filters and Cu$K\alpha$ radiation, using 30 kV and 20 mA, calibrated with silicon, at a 2°/min rate.

Infrared (IR) spectra were recorded in a Perkin Elmer 1600 Fourier transform spectrometer, using nujol dispersions between alkali halide windows.

Scanning electron microscopy (SEM) micrographs were obtained in a JEOL, model JSM T-300, microscope, from gold coated dispersed powder samples.

X-ray fluorescence measurements were carried out in a Tracor mod. Spectrace 5000, analyzed with the fundamental parameters method.

Differential thermal analysis (DTA) measurements were performed in a Shimadzu 50WS thermal analyzer, under air flow at 50 ml/min and a 5 °C/min heating rate, up to 1000 °C.

3. Results

3.1. α-$Ba(FeS_2)_2$

X-ray diffraction patterns of the heated α-$Ba(FeS_2)_2$ samples are shown in Fig. 1. The compound is stable up to 300 °C. At 320 °C, a complete breakdown on the original structure took place, leading to $BaSO_4$ and FeS_2 (pyrite).

At higher temperatures the pyrite was oxidized to α-Fe_2O_3. A mixture of α-Fe_2O_3 and $BaSO_4$ was obtained at 500 °C. Further heating to higher temperatures up to 1000 °C caused no additional changes.

IR spectroscopy measurements confirmed our XRD data. The α-$Ba(FeS_2)_2$ spectrum does not show any features in the 4000–400 cm^{-1} range. The sample heated to 500 °C presented vibrations attributed to SO_4^{2-} ions at 1170, 1115, 1063 (ν_3)*, 982 (ν_1), 636, 610 (ν_4) and 468 cm^{-1} (ν_2) in $BaSO_4$ [11] together with Fe-O bands at 570, 530, 476, 445 cm^{-1} (* ν_1: symmetric stretching mode; ν_3: asymmetric stretching mode; ν_4: in-plane deformation) [12].

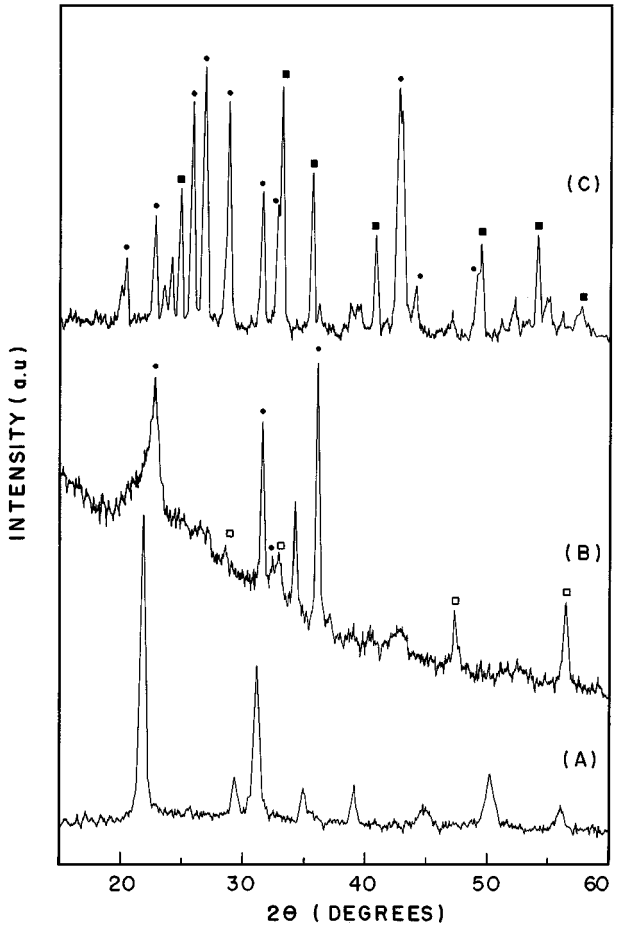

Figure 1 XRD patterns for (A) α-$Ba(FeS_2)_2$ and heat-treatment products obtained after 2 hours at (B) 320 °C and (C) 500 °C. The observed peaks were assigned to: (●) $BaSO_4$, (□) FeS_2 and (■) α-Fe_2O_3.

A scanning electron micrograph of α-$Ba(FeS_2)_2$ is shown in Fig. 2A. This solid displays a fibrous morphology consistent with its quasi-unidimensional character. The fibers are very thin (1 to 2 μm). However, the stacking of the precursor $KFeS_2$, reported elsewhere, was completely removed [10]. Other morphologies that could be associated with the decomposition products α-Fe_2O_3 and $BaSO_4$ were not observed and the fibrous pattern was maintained up to 700 °C, as showed by Fig. 2B.

3.2. $AgFeS_2$

Fig. 3 presents the thermal decomposition of $AgFeS_2$ under air atmosphere, as studied by XRD. At 200 °C two new sets of reflections indexed as FeS_2 (pyrite) and Ag_2S were observed. Some features of the original $AgFeS_2$ sample are still present up to 300 °C.

Samples treated at 400 °C showed the oxidation of FeS_2 and Ag_2S to α-Fe_2O_3 and Ag_2SO_4 respectively. Between 500 and 800 °C metallic silver is formed as a product of silver sulfate decomposition. The final products is a mixture of α-Fe_2O_3 and metallic silver, which particles are clearly distinguished by the naked eye.

Infrared spectroscopy experiments were carried out in the 1300–250 cm^{-1} range for the samples heated up to 300 °C and between 1300 and 400 cm^{-1}, for the samples heated to 400–1000 °C. The data are summarized in Table I. The spectrum of the sample heated to 300 °C already showed Fe-O vibrations, but XRD measurements did not detect Fe_2O_3 in the samples heated to this temperature.

Scanning Electron Microscopy showed that the fibrous character of the $KFeS_2$ precursor is lost on the formation of $AgFeS_2$, as presented in Fig. 4A. The crystals do not present any definite pattern. Segregation of different phases could not be observed as the heat treatment was carried out. Only samples heated to 800 °C showed two different morphological features (Fig. 4B). The large, smooth and flat surface corresponds to the metallic silver and the little agglomerated particles, to α-Fe_2O_3.

3.3. Thermal analysis

The DTA curves for $Ba(FeS_2)_2$ and $AgFeS_2$ are presented in Fig. 5. All events observed were endothermic.

TABLE I IR frequencies (1300–250 cm^{-1}) for $AgFeS_2$ samples heated at different temperatures [11–13]

Wavenumber (cm^{-1})			Tentative assignment
300 °C	400 °C	800 °C	
241, 252			Ag-S
296, 349, 410			Fe-S
320, 378, 474	462, 535	464, 561	Fe-O
	594, 606		$\nu_3(SO_4^{2-})$
	1059	1054	$\nu_4(SO_4^{2-})$

ν_3: asymetric stretching mode, ν_4: in plane deformation.

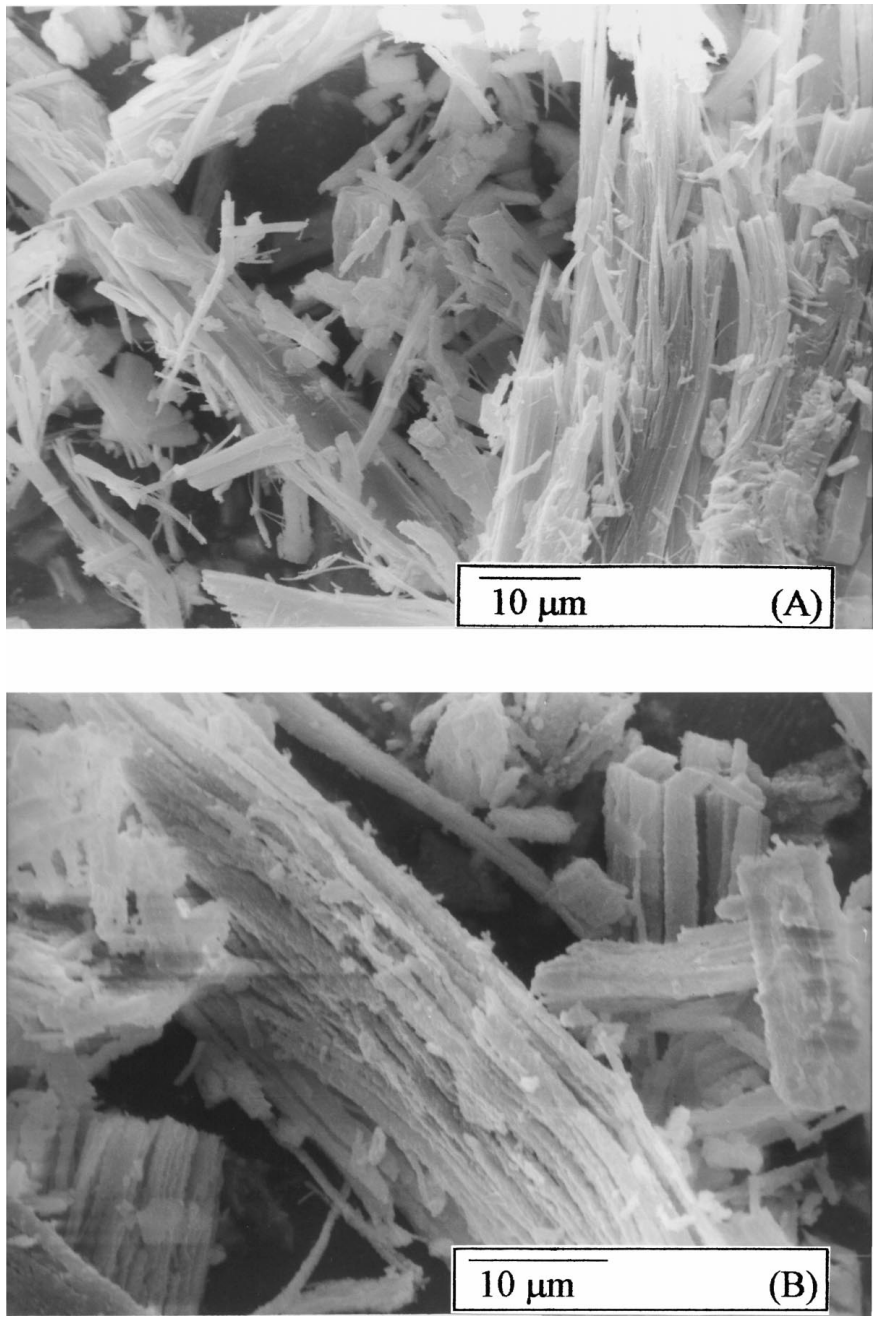

Figure 2 Scanning electron micrographs of (A) α-$Ba(FeS_2)_2$ (1500×); (B) α-$Ba(FeS_2)_2$ heated at 700 °C for 2 hours (2000×).

Three sets of endothermic peaks could be observed at 400, 425 and 450 °C for α-$Ba(FeS_2)_2$. It is difficult to assign each peak individually because there are several concurrent heat transfer events in a narrow temperature range and all of these events are closely related. The first step must be the breakdown of the pristine structure, which is followed by pyrite formation. Next, oxygen diffuses through the crystals and FeS_2 is oxidized to Fe_2O_3, and almost simultaneously, sulfide ions are oxidized to sulfate. $BaSO_4$ is detected and the sulfur excess evolves from the system, probably as SO_2. The wide peak ranging from 450 to 800 °C derives from the crystallization of α-Fe_2O_3 and $BaSO_4$, in agreement with the increase of the intensities of the reflections observed by XRD, up to 800 °C.

$AgFeS_2$ DTA curve closely agrees with the results obtained on the static heat treatments. The first transition at 210 °C represents the breakdown of the chalcopyrite structure, leading to the metal sulfides. The second peak at 370 °C was assigned to the oxidation of these sulfides, followed by crystallization, again confirmed by a wide peak ranging from 400 to 750 °C. This peak must also reflect the decomposition of $AgSO_4$ to metallic silver. Finally, a transition at 825 °C was attributed to silver crystallization.

4. Discussion

From the data discussed above, we observed that α-$Ba(FeS_2)_2$ is thermally more stable than $AgFeS_2$. This could be explained by the diffusional processes involved in the reaction of each compound. In the formation of $AgFeS_2$, alternate iron atoms in Fe-S chains drop out simultaneously with K^+ exchange by Ag^+ [14]. The

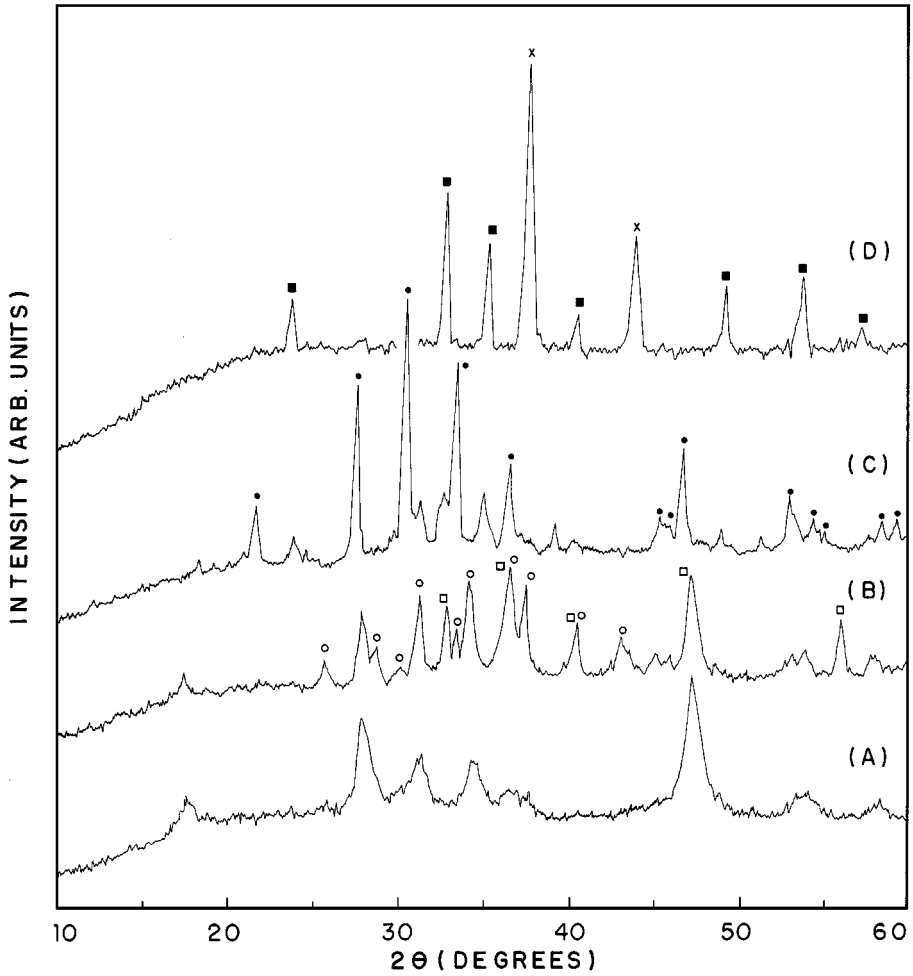

Figure 3 XRD patterns for (A) $AgFeS_2$, and heat-treatment products obtained after for 2 hours at (B) 200 °C, (C) 400 °C and (D) 800 °C. The observed peaks were assigned to: (○) Ag_2S, (●) Ag_2SO_4, (□) FeS_2, (■) α-Fe_2O_3, (×) Ag.

displacement of the atoms within the crystal structure is greater in $AgFeS_2$, as a 3D network results from a quasi-unidimensional compound. In the case of the exchange of potassium ions with barium, there is only a rearrangement of the original chain structure. Hence, the compound derived from more extensive rearrangement on the precursor structure, namely $AgFeS_2$, shows poorer thermal stability.

The first step of α-$Ba(FeS_2)_2$ thermal decomposition with the initial formation of pyrite and the alkaline earth sulfate is similar to that observed for $KFeS_2$, described in our earlier paper [10].

The formation of Ag_2S and FeS_2 through the initial decomposition of $AgFeS_2$ seems to be a typical example of internal thermal reactions, as described by Stoch [15], in which a diffusional displacement of atoms and ions occurs over distances greater than the crystal lattice parameters, leading to a redistribution of the chemical components and to the synthesis of new products, but part of the structural framework and the outershape of the parent substance are preserved, as we observed by SEM.

The oxidation of pyrite (FeS_2) to hematite (α-Fe_2O_3) at 400 °C is consistent with the results by Jorgensen and Moyle [16], who proposed the reaction:

$$2FeS_2 + \frac{11}{2}O_2 \rightarrow Fe_2O_3 + 4SO_2 \qquad (1)$$

This occurs simultaneously with the oxidation of silver sulfide to silver sulfate, showing that this second step of the decomposition is characterized by the diffusion and reaction of O_2 through the crystals. The decomposition of Ag_2SO_4 to metallic silver in the presence of SO_2, was described by Hegedüs and Fukker [17] at temperatures higher than 350 °C. In this case, SO_2 is provided by pyrite oxidation as stated by Equation 1.

The thermal behavior of $AgFeS_2$ is markedly different from its structural analogue chalcopyrite, $CuFeS_2$, where a Cu_4FeS_5 phase plus iron oxide were observed instead of metallic sulfides in the beginning of the process. Another difference is the formation of the $CuFe_2S_4$ as one of the final decomposition products of heat-treated chalcopyrite [18].

The results obtained from static experiments closely agree with dynamic DTA. All decomposition steps observed on XRD measurements could be assigned to the events observed in DTA. The high temperature wide peaks represent the crystallization of the final products.

The 3D network of $AgFeS_2$ with all atoms in tetrahedral sites shows a considerable covalence between these *d-block* metals and sulfur atoms, hence, M-S distances are shorter in this compound. Thus, rearrangement of the structure to metal sulfide formation is feasible and the formation of these compounds proceeds under air atmosphere at moderate temperatures.

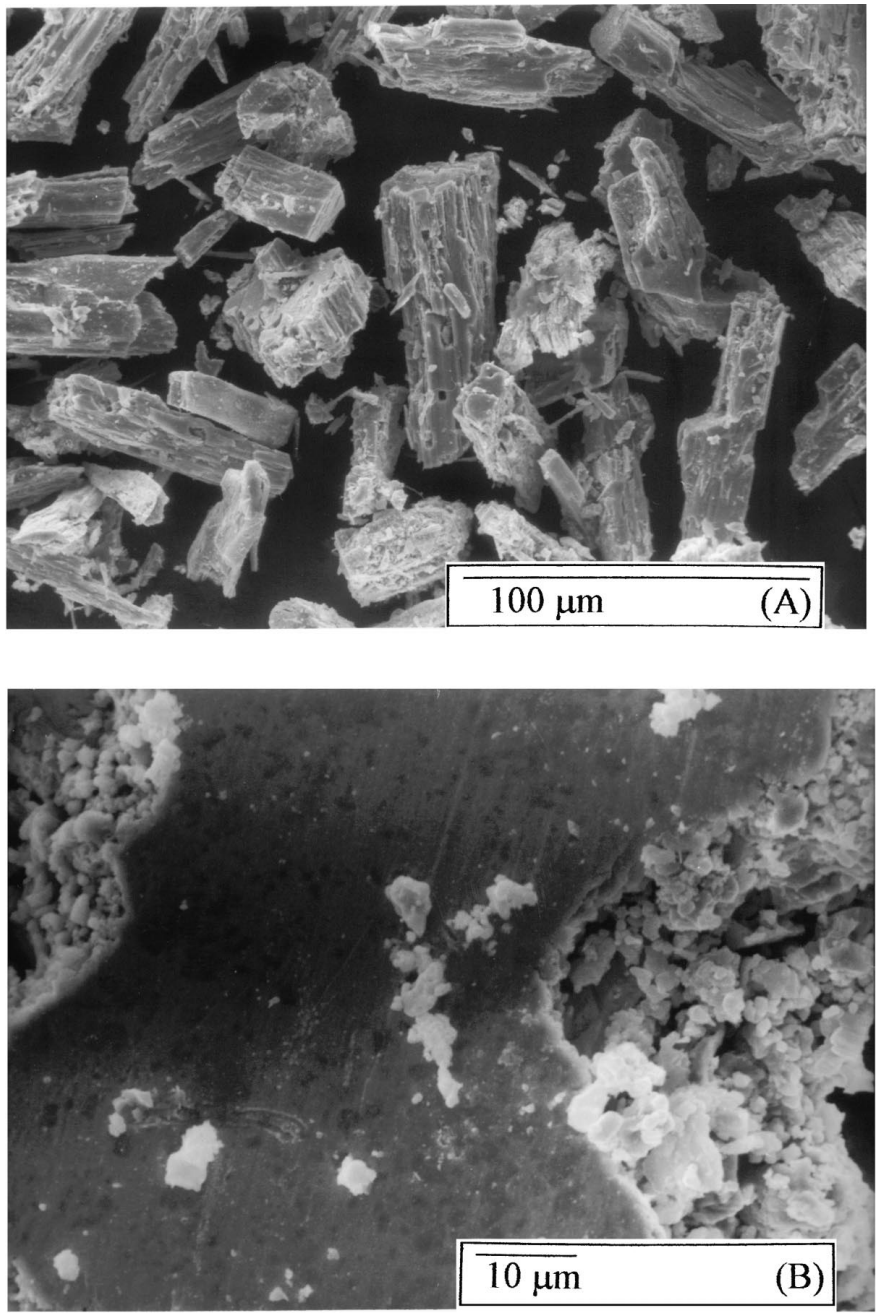

Figure 4 Scanning electron micrographs for (A) $AgFeS_2$ (500×) and (B) $AgFeS_2$ heated at 800 °C for 2 hours (1500×).

TABLE II Metal-sulfur distances in α-$Ba(FeS_2)_2$, $CuFeS_2$[a] and $KFeS_2$

Compound	M-S distance (Å)	Fe-S distance (Å)
α-$Ba(FeS_2)_2$	3.43	2.32
$KFeS_2$	3.33–3.48	2.20, 2.28
$CuFeS_2$	2.32	2.20

[a]M-S distances for $AgFeS_2$ are not available, but this compound is isostructural with $CuFeS_2$. Their cell parameters differ only in the *a* value that is 5.66 Å for $AgFeS_2$ and 5.24 Å for $CuFeS_2$. We assumed that M-S distances for silver iron sulfide are slightly greater than for chalcopyrite.

In quasi-unidimensional compounds like α-$Ba(FeS_2)_2$ and $KFeS_2$, the alkaline or alkaline earth atoms act as counter-ion to the $(FeS_2)_n^{n-}$ chains, in a more opened lattice. Metal-sulfur distances for these compounds are summarized in the Table II.

To sum up, when the metallic ion is more closely packed with sulfur, the decomposition starts with the formation of the metallic sulfides. When this distance is about 3.30 Å, the metallic sulfate is directly formed at the beginning of the thermal decomposition by oxygen diffusion through the system.

5. Conclusions

The thermal decomposition of α-$Ba(FeS_2)_2$ leads to FeS_2, α-Fe_2O_3 and $BaSO_4$ up to 500 °C. Ag_2S, FeS_2, Ag_2SO_4, α-Fe_2O_3 and metallic silver are formed during the decomposition of $AgFeS_2$, which starts near 200 °C and ends at 800 °C. The formation of metallic sulfides or sulfates can be correlated with the metal to sulfur packing, distances and interactions in the parent materials. The results of static and dynamic heating experiments are in close agreement, each peak of the

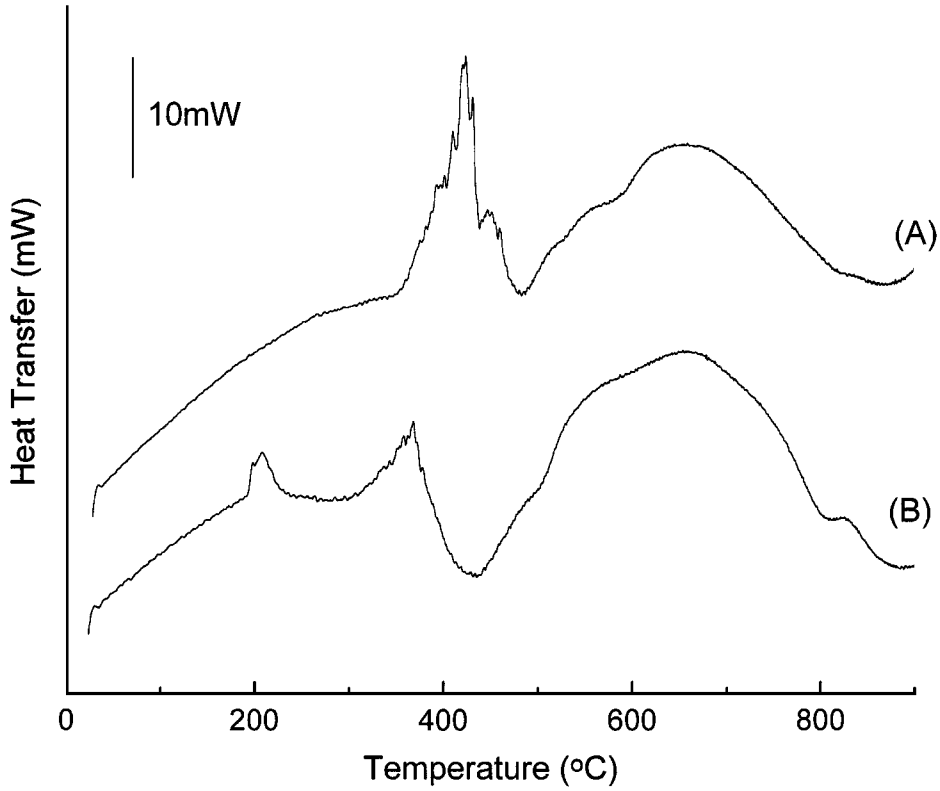

Figure 5 DTA curves for (A) α-$Ba(FeS_2)_2$ and (B) $AgFeS_2$.

thermograms could be assigned to the formation of new compounds or crystallization of these products. Morphological modifications resulting from ion exchange of barium and silver with potassium ions on $KFeS_2$ were presented for the first time.

References

1. J. W. BOON and C. H. MACGILLAVRY, *Recl. Trav. Chim. Pays Bas* **61** (1942) 910.
2. D. C. JOHNSTON, S. C. MRAW and A. J. JACOBSON, *Solid State Commun.* **44** (1982) 837.
3. J. ZINK and K. NAGORNY, *J. Phys. Chem. Solids* **49** (1988) 1429.
4. W. V. SWEENEY and R. E. COOFMAN, *Biochim. Biophys. Acta* **286** (1972) 26.
5. A. J. JACOBSON, M. S. WHITTINGHAM and S. M. RICH, *J. Electrochem. Soc.* **126** (1979) 887.
6. H. BOLLER, *Monatsch. Chem.* **109** (1978) 975.
7. J. W. BOON, *Recl.: Trav. Chim. Pays-Bas* **63** (1944) 69.
8. R. PACKROFF and H. H. SCHMIDTKE, *Inorg. Chem.* **32** (1993) 654.
9. I. E. GREY, *J. Solid State Chem.* **11** (1974) 128.
10. A. GALEMBECK and O. L. ALVES, *Materials Letters* **23** (1995) 133.
11. F. A. MILLER, G. L. CARLSSON, F. F. BENTLEY and W. H. JONES, *Spectrochim. Acta* **16** (1960) 135.
12. B. GILLOT, F. BOUTON, F. CHASSANGNEUX and A. ROUSSET, *J. Solid State Chem.* **33** (1980) 245.
13. H. D. LUTZ. G. KLICHE and H. HAEUSLER, *Z. Naturforsch.* **36a** (1981) 184.
14. A. F. WELLS, "Structural Inorganic Chemistry" (Oxford University Press, 1984) p. 777.
15. L. STOCH, *J. Thermal Anal.* **40** (1993) 107.
16. F. R. A. JORGENSEN and F. J. MOYLE, *ibid.* **29** (1984) 13.
17. HEGEDÜS and FUKKER, *Z. Anorg. Allgem. Chem.* **284** (1956) 20.
18. K. TKÁCOVÁ, P. BALÁZ and T. A. KORNEVA, *J. Thermal Anal.* **34** (1988) 1031.

Received 1 August 1997
and accepted 22 January 1999